DOE/ET/20460-3

AMORPHOUS SILICON THIN FILM HETEROJUNCTION SOLAR CELLS

Third Quarterly Progress Report for April 1—June 30, 1979

August 1, 1979

Work Performed Under Contract No. ET-78-C-03-1846

Mobil Tyco Solar Energy Corporation
Waltham, Massachusetts

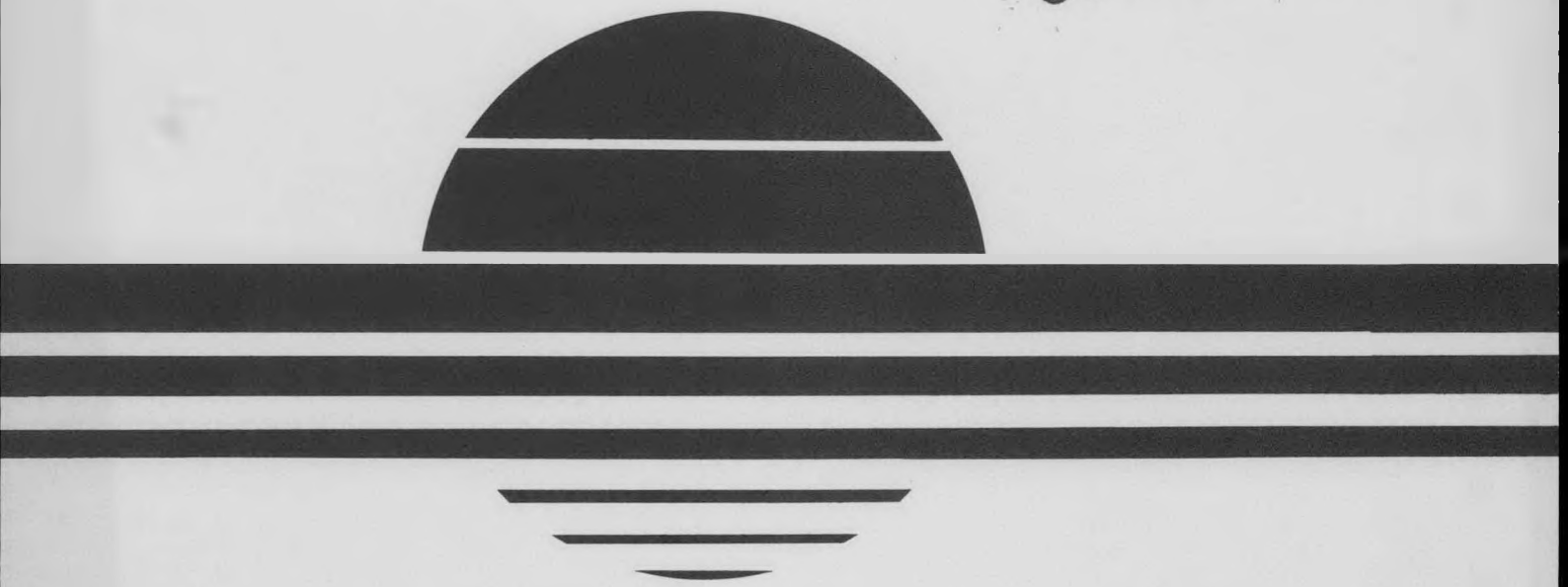

U.S. Department of Energy

Solar Energy

NOTICE

DOE/ET/20460-3

AMORPHOUS-SILICON THIN-FILM HETEROJUNCTION SOLAR CELLS

Third Quarterly Progress Report for April 1—June 30, 1979

DOE/ET/20460--3

DE83 013418

August 1, 1979

Work Performed Under Contract No. ET-78-C-03-1846

MASTER

Mobil Tyco Solar Energy Corporation
Waltham, Massachusetts

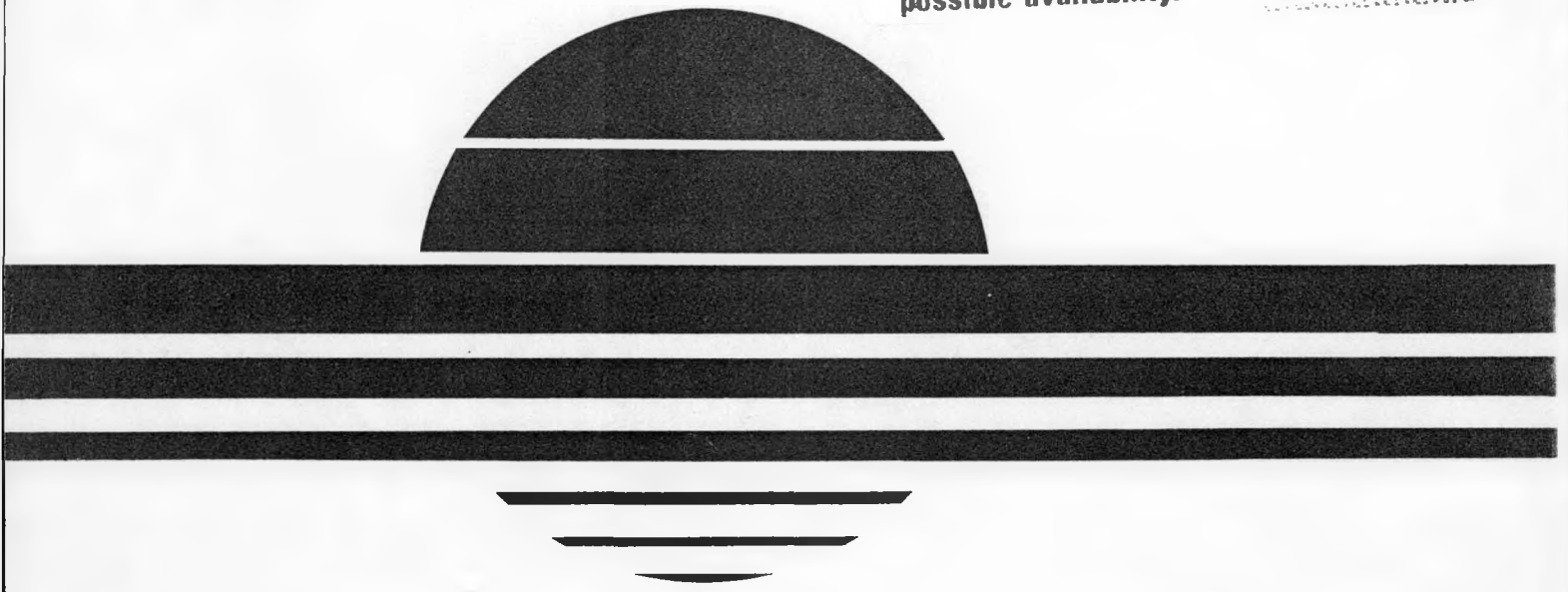

U.S. Department of Energy

Solar Energy

MT-79-3Q

DOE/ET/20460-3
Distribution Category UC-63e

Mobil Tyco Solar Energy Corporation

THIRD QUARTERLY PROGRESS REPORT
1 April - 30 June 1979

Contract Title and Number
Amorphous Silicon Thin Film
Heterojunction Solar Cells
DE-AC03-79 ET20460

August 1, 1979

INTRODUCTION

We here report additional results of the experiments of the substitution of C for Si and initial results on the substitution of Ge for Si in hydrogenated a-Si films grown by capacitive glow discharge techniques. Our results for the Group IV matrix substitutions are qualitatively consistent with the published data for the hydrogenated a-Si_xC_{1-x} [1-5] and the a-Si_xGe_{1-x} [6,7] systems. In this report we also summarize the electrical properties of the various films measured thus far.

GROWTH OF FILMS

For all experiments, we have maintained the glow discharge parameters as consistent as possible with those which were determined for the reproducible preparation of a-Si(H) films in our apparatus. The apparatus was described in detail in the preceding quarterly report.[8] The deposition parameters are:

P: 0.5 Torr; reactants, e.g., SiH_4, (10%) diluted with H_2 (30%) and Ar (60%).
Gas Flow: 20 sccm
Substrate Temperature: 200°C
Power Input: <15 Watts (8×10^{-2} W/cm^2 of electrode area)

These conditions result in a deposition rate for the a-Si(H) of 2-3 Å/sec. a hydrogen incorporation of 16%, and an optical energy gap of 1.76 eV.

Si-C

The source of carbon used for all these experiments is ethylene (C_2H_4). The SiH_4 and C_2H_4 are fed separately to the g.d. region through quartz tubes

designed for thorough mixing of the gases at the nozzle exits. The volume percent for the combined gases is maintained at the same 10% used for the a-Si(H) growth with H_2 and Ar as the usual diluents. Deposition rates were about 1-2 Å/sec and thicknesses were .5 to 1.2 μm.

Electron microprobe analyses of these samples indicated they were inhomogeneous in C concentration across the film, however, the samples were too thin to obtain meaningful quantitative determinations.

In an attempt to improve the deposition rate, while at the same time exploring the doping of a-$Si_{1-x}C_x$, we prepared a set of samples using no H_2 or Ar dilution, a gas-flow ratio of C_2H_4/SiH_4 of 2, and an addition of 1% B_2H_6 to the SiH_4. This did increase the rate of deposition to 3-4 Å/sec and led to significant changes in the optical and electrical properties which are discussed below. More samples of 4-5 μm thickness are being grown under these conditions for further electron microprobe analysis and property measurements.

Ge-Si

Films of a-$Si_xGe_{(1-x)}$(H) have been deposited using the same discharge conditions as above. The germanium source is only 2% GeH_4 in Ar which results in dilution of the reactants to <10%; additionally we are limited to Ge/Si ratios <1 if we maintain a total flow of 20 sccm. We will be receiving an 100% germane source; in the meantime we have prepared films from Ge/Si ratios of 0.02, 0.08 and 0.7 in the gas feed. At the 0.02 concentration ratio, deposition rates were enhanced to ~10 Å/sec. At the 0.08 ratio, rates diminished to 2-3 Å/sec, while at the 0.7 ratio, growth rates were down to 0.7 Å/sec. These growth rates are slower than those reported by Chevallier, et. al.[6] and are most likely a consequence of the dilute reactant concentration.

Sn-Si

Efforts to substitute Sn for Si by resistively heating Sn above its melting point and entraining the vapor in the argon gas stream have so far not been successful. The Sn-Si was deposited as an opaque film with metallic inclusions. A selection of alkane-Sn substances has been obtained including tributyl tin hydride and tetramethyl tin. These sources for tin will be used if our experiments with resistively heated Sn for a Sn vapor source for g.d. continue to present difficulties. These compounds will allow us to explore the simultaneous substitution of Sn and C for the silicon in a-Si(H).

OPTICAL CHARACTERIZATION

Si-C

The IR vibrational spectra of these materials are similar to those obtained by Wieder, et. al.[4] An interesting feature of these spectra is that even at the lowest gas volume concentration ratio of C/Si, i.e., 0.13, the stretching mode for Si-H is shifted from 2000 cm^{-1} to ~2080 cm^{-1}. The vibrational bands for this and other C/Si ratios are given in Table I.

The calculation of optical constants (near the absorption edge) in the various amorphous films is made following the procedure evaluated and outlined by D. Yates here at MTSEC. The details of the evaluation are contained in the Appendix to this report.

The optical energy gap for these compounds was obtained from the extrapolation of the linear portion of the $(\alpha h\nu)^{\frac{1}{2}}$ versus energy $(h\nu)$ curve. The change in gap with C concentration is shown in Fig. 1a. These points are not in correspondence with those obtained by Anderson and Spear[1]; this is not surprising since both the concentration of reactants and the deposition parameters for our system are quite different from theirs.

Both from differences such as the above and from observations in our system with a-Si(H), it is clear that the samples, structurally and compositionally, can be affected by not only the deposition parameters and by alloying, but also by the presence of residual impurities in the chamber and by certain doping elements.

We have noted above, the shift in the 2000 cm^{-1} Si-H stretch band with the addition of C. We have also observed this shift to a higher wave number or the presence of a double peak at ~2100 cm^{-1} and 2000 cm^{-1} in a-Si(H) when we have one or more of the following conditions.

a. doping with B_2H_6 at any concentration (but not with PH_3)
b. evidence of carbon contamination (peak appearing at 785 cm^{-1}), probably due to incomplete removal of organic degreasing solvents.
c. oxygen contamination (band appearing at ~990 cm^{-1}),[9], and
d. deposition parameters which produce a polysilane deposition (powdery deposit) in the chamber.

In our original determination of deposition parameters we selected those conditions which gave us reproducibly an IR vibrational spectrum displaying uniquely the peaks at 2000 cm^{-1} and 640 cm^{-1}, the stretch and wag modes of SiH respectively. This IR criterion was based on the published data [10] supporting the observation that the free electron spin density was inversely related to the ratio of the absorption coefficients at 2000 cm^{-1} and 2100 cm^{-1}.

The occurrence of the 2100 cm^{-1} peak is widely reported as correlated with poor device properties, whatever the source of the peak. Since we obtain the 2000 cm^{-1} peak apparently without inclusion of higher frequency contributions in our a-Si(H) we are investigating the possible correlation of the effects of the SiC or the residually contaminating impurities, i.e., C/Si << .1, on the device and photoconductive properties. Additionally, since P (heavy element) does not result in changes in the IR spectrum while the addition of N (a light element comparable to B) does [11,12] then use of a heavier acceptor atom for doping may also affect the electrical and optical properties in a manner analagous to P.

In view of the hydrogen evolution results described in the Xerox report [13] it would be informative to determine the hydrogen vs. temperature evolution spectrum for the a-Si(H) with bands at 2000 cm^{-1}, and/or 2080 cm^{-1} and the B doped films with the (2000 cm^{-1}, 2100 cm^{-1}) doublet.

Si-Ge

These films have had only a preliminary examination. The change in energy gap with Ge concentration is shown in Fig. 1b. The films obtained at the Ge concentration of 0.02 and .08 have been sent for electron microprobe analysis.

MATERIAL CHARACTERIZATION

Additional analytical characterization has included optical microscopy of a fractured cross-section of a 2μm thick film. At 2000X no structure with the columnar features described by Knights [10,13] was discernible. A sample prepared for the SEM also did not show any regular structure of the type described even at magnifications of 10 KX. An n-i-p structure and an n-doped film both on Mo substrates have been prepared to investigate the possibility of determining the minority carrier diffusion length with the scanning electron microscope using techniques such as those described by Partain and Shea.[14]

ELECTRICAL MEASUREMENTS

The dark conductivity and photoconductivity of samples of a-$Si_xM_{(1-x)}$(H) have been measured as a function of temperature, level of illumination and for M = C, Ge. Usually, the conductivities are deduced from measurements of current vs. voltage or voltage drop vs. position on samples with coplanar metal contacts as shown in Fig. 2. The metal pads are separated by an a-$Si_xM_{(1-x)}$(H) film, 0.8 cm wide, 0.1 cm long, and approximately 10^{-4} cm thick.

Although there is a contact resistance at the metal-amorphous semiconductor interface, there does not appear to be any dependence of contact characteristics on contacting metal where Cr, Au, Al, and Pt have been employed. Lower resistivity samples ($\approx 10^4$-10^2 Ω-cm) appear to have the lowest contact resistances.

To determine the resistivity of the films it is necessary to remove the influence of the contacts from the measurement. As can be seen in Figs. 3 and 4, the I vs. V characteristic is not necessarily linear, although the electric fields imposed are modest (≈200 V/cm). That is, one or both of the contacts are blocking. However, since the I vs. V characteristic is nearly symmetric about the origin, as seen in Fig. 4, the contact between the metal and semiconductor appears to be the same beneath both metal pads for a given sample. As shown in Fig. 4, the shape of I vs. V characteristic is roughly the same in the dark (D) or under fluorescent (room) light (FL).

Considering the voltage drop across the a-Si(H) as a function of position between the contacting pads, as in Figs. 5b and 5c, it is apparent that the electric field in the linear portion of V vs. d is proportional to the current going through the sample (Fig. 5a). Similar proportionality is observed in a sample that is highly non-linear in I vs. V, thus implying the contacts are of a blocking nature and are in series with the ohmic a-Si(H). An alternate means of determining the resistivity of a sample is by employing the reciprocal of the slope of the I vs. V plot if this I vs. V characteristic is nearly linear. Neglecting the contact resistance in this way underestimates the resistivity of the sample by 10-20%.

Although the plots of V vs. d are not affected by the fluorescent light, illumination approximating AM1 causes large changes. This can be seen in Fig. 6 where the D and FL points are coincident while those obtained under AM1 show a much higher drop at the metal-semiconductor interface on the low voltage end of the gap. A higher level of illumination and consequent higher photoconductivity could require the reverse biased contact to have a higher potential drop across it to allow a higher current to flow. An alternate explanation involves a

Schottky barrier being established at the contacts and influencing V vs. d. This possibility is being examined by using thicker metal contacts and collimating the light beam.

A sandwich contact geometry has also been used on a-Si(H) samples and the dark resistivity obtained from I vs. V of these samples was found to be several orders of magnitude higher than the resistivities of films from the same deposition run using coplanar contacts. Since the coplanar contact samples have resistances that scale with the thickness of the a-Si(H) film, thereby ruling out a gross surface conductance effect in these samples, the resistivities obtained from the sandwich geometry contact samples are considered questionable. For this reason the coplanar geometry has been used to determine the conductivity of our samples.

Measuring the photoconductivity of the samples is somewhat more tenuous since complications due to photovoltages or trapping effects may arise; furthermore, there appear to be light induced changes in the photoconductivity and dark conductivity at illumination levels near AM1. Illumination at AM1 decreases the dark conductivity by a factor of two to four per hour over a period of ≈ two hours. This rate of decrease is approximately the same as observed at RCA.[15] RCA also determined that annealing near 150°C overnight in the dark restored the original conductivity; this also occurred for our samples but contrary to RCA's observations, "annealing" the samples at room temperature overnight increased the conductivity of the samples towards, but not attaining, the original conductivity. The RCA samples were fabricated at 300°C while those tested here were deposited at 200°C. The difference in structure might be such that the films deposited at lower temperatures allow diffusion to take place at a much higher rate.

The film resistance as a function of temperature up to approximately 250°C was also measured by heating the stage on which the samples were mounted.

Si

The resistivities of the a-Si(H) samples at room temperature in the dark and under AM1 illumination are given in Table II. With the exception of samples from run A-27 the resistivities in a given run are the same within a factor of three. The low resistivity of A-27-3 may have been due to a growth related in-

stability since it later spalled off the substrate. The resistivity of A-34-5 has been determined for the entire cross section of the film, not for the p- or n-type layers, consequently the resistivity of one of these layers must be less than the value given in Table II. The values for the dark resistivity of the samples correspond very well to those produced by Spear and LeComber as a function of doping level.[16] The difference in resistivity of films from runs A-13 and A-32 may be related to differences in deposition conditions, leading to structural changes.

A plot of the logarithm of sample conductivity versus 1/T is shown in Fig. 7. The logarithm of the dark conductivity increases nearly linearly with an activation energy of 0.80 eV. At higher temperatures the conductivity increases at a less than exponential rate, an effect seen by many other groups and which lacks an adequate explanation.[12] On cooling, however, the samples rarely retrace their original values of log σ vs. 1/T, instead a curve with a slope corresponding to $\Delta E_a \approx .2$ eV is followed; on reheating the curve observed on cooling is retraced. The plot of log σ versus 1/T is also shown in Fig. 7 for illumination with fluorescent light. The dependence is not exponential for this sample and σ_{FL} eventually merges with the dark current. On cooling the conductivity is again higher than initially and has a slope corresponding to an activation energy of $\sim$ .2 eV also, suggesting at a high enough temperature the carriers are provided by thermal excitation and not photo-excitation. It is worth noting that the slope of the plot for the undoped samples in the dark corresponds to an activation energy of .8 eV, which with the optical gap of these samples $\approx$ 1.8 eV, suggests the samples may be near intrinsic. Doped films, on the other hand, have activation energies around .34 eV for the highest doping levels, as in Fig. 8. This last value is somewhat larger than reported in the literature;[16] this difference is being investigated.

The dark conductivity at low temperature is changed after heating to temperature in excess of 90^{o}C. This change implies the film has either annealed or reacted with its environment in some way to produce a material with a Fermi level closer to one of the band edges than initially or to enhance conduction near the Fermi level in the a-Si(H). Taken along with the recovery of AMJ illuminated samples annealed overnight this change in resistivity with annealing implies the films are susceptible to change at moderate temperatures, due to either annealing or reaction with, say, water vapor. Further effort will be directed at determining the nature and time-at-temperature dependence of this susceptibility since it could influence solar cell characteristics and behavior.

SiC

The dependence of log σ vs. 1/T for a sample prepared from a discharge containing 3.2% SiH_4 and 6.8% C_2H_4 is shown in Fig. 9. The dark conductivity data between 50°C and 200°C can be fit fairly well with an activation energy of 1.0 eV. This activation energy and the lower conductivity of this sample, which is presumably due to a larger energy gap, agrees well with previous work.[1] On cooling this sample showed the same conductivity as on heating, unlike the a-Si(H) films, indicating an increased resistance to changes upon annealing or reaction with the environment.

Other samples, prepared with higher C_2H_4/SiH_4 concentrations, yielded resistivities too high to be measured by our present techniques; our experimental apparatus is being altered to determine the resistivity of these samples. The films prepared with a low C_2H_4/SiH_4 ratio possessed resistivities very close to those of a-Si(H), as seen in Table II.

Samples from run A-12 indicate the dark conductivity of a-$Si_xC_{(1-x)}$(H) can be increased substantially by doping, in the cases under consideration from 10^{11} to 10^8 Ω-cm by introducing diborane into the glow discharge. The AM1 resistivity appears to be higher upon doping, although this might be related to other changes made during runs A-12 and A-25. These data should not be considered the optimum for the system and the effects of doping a-$Si_xC_{(1-x)}$(H) are being pursued.

SiGe

Table II also includes preliminary data on the films produced from SiH_4-GeH_4 mixtures (run A-37 GeH_4/SiH_4 = 0.02 and run A-38 GeH_4/SiH_4 = 0.08. These samples give a resistivity for the films containing Ge which is the same or higher than films produced from SiH_4 alone. This increase in resistivity of samples may be due to impurities or inhomogeneities deposition rather than to the effects of Ge substitution. The problem of deposition is being addressed by modifying the geometry of the reaction vessel and gas feed lines by increasing the concentration of reactants in the gas flow. The consideration of impurity contamination may be resolved by the electron microprobe analysis and/or the IR spectra of these samples.

SUMMARY

The apparatus for measuring the conductivity of the samples at room temperature is operational and the conductivities and photoconductivities of samples made under a number of conditions, including Ge and C incorporation, have been measured. These measurements are in very good agreement with the literature, yielding dark conductivities between 10^9 and 10^2 Ω-cm, depending on doping level.

The dark conductivity of undoped samples exhibits an activation energy of 0.8 eV and undoped samples containing large amounts of C have an activation energy of 1.0 eV.

Heating the samples to temperatures in excess of 90°C appears to increase the conductivity near room temperature due to either a change in the Fermi level or enhancement of conduction at the Fermi level. Illumination levels near AM1 gradually reduce the conductivity of the samples although these changes can be recovered by annealing overnight at 150°C or partly recovered by annealing at room temperature. Further work is underway to determine the nature of these changes upon heating and under illumination and their effect on solar cell behavior.

PLANS FOR NEXT PERIOD

We will continue the investigations with the Group IV substitutions, initiate preliminary experiments with the alkali metal substitutions for H and if time allows, we will also explore the use of heavier elements, e.g., Al, Ga, perhaps In, as dopants in place of B. For these materials, as well as for the Sn, we are designing an alternative heating arrangement to the simple resistively heated boat which we have been using in our trials with Sn. Our intent is to improve the control of introduction and concentration of the vapor species of these materials.

We are providing samples as indicated above for hydrogen vs. temperature evolution spectra determinations by Professor W. Paul's group at Harvard University. It would also be worthwhile to provide samples for a quantitative analysis of the 2000 cm^{-1} peak we ordinarily obtain using the Fourier Transform capability in Professor Paul's group to determine if any other absorption band component contributes to this peak.

The measurements of photoconductive and device characteristics will continue with increased emphasis on device properties, particularly with heterojunction devices.

TABLE I

C/Si Vol.* Ratio	Stretching C-Hn	Stretching Si-H	Vibrational Frequencies (cm^{-1}) †				
			Bending $Si-CH_3$		Rocking C-Hn	Wagging $Si-CH_3$	Wagging SiH
			Anti Sym.	Sym.			
1.85	2950 2908 2865	2110	1450 1400	1250	1000 970	795	630
1.45	2950 2900 2870	2103	1450 1400	1250	1000	785	620
0.13	2940 2870	2090	††	††	960 890†† 850††	770	640
0.0		2000					635

* Gas flow is 90% H_2 + Ar; 10% (C_2 + SiH_4)

† Designation adopted are those of ref. 4.

†† Other peaks observed in this region are too weak and convoluted to identify. Ref. 4 suggests these bands may result from mixed modes containing a mixture of Si-C stretch and an opening of the C-H bond angle.

TABLE II

Sample	Matrix	Dopant	Resistivity (Ω-cm) Dark	AM1	Hydride Concentration in Gas	
			a-Si(II)			
A-18-9	Si		6.0×10^9	6.2×10^4	10% SiH_4	
A-20-9	Si		3.3×10^9	1.0×10^5	10% SiH_4	
A-21-1	Si		4.3×10^9		10% SiH_4	
A-27-1	Si		2.6×10^9	6.2×10^4	10% SiH_4	
A-27-3	Si		3.4×10^8		10% SiH_4	
A-31-5	Si		2.2×10^9	1.0×10^5	10% SiH_4	Remainder H_2 + Ar
A-35-5*	Si		1.3×10^8	1.3×10^6	10% SiH_4	Remainder H_2 + Ar
A-13-1	Si	P	9.2×10^4	3.2×10^4	1% PH_3 in 10% SiH_4	
A-13-5	Si	P	1.2×10^5		1% PH_3 in 10% SiH_4	
A-32-5	Si	P	2.8×10^2	2.5×10^2	1% PH_3 in 10% SiH_4	
A-35-5	Si	B	7.0×10^8	2.4×10^5	.1% B_2H_6 in 10% SiH_4	
A-33-9	Si	B	2.5×10^8	1.4×10^5	.1% B_2H_6 in 10% SiH_4	
A-36-5	Si	B	1.2×10^5		.5% B_2H_6 in 10% SiH_4	
A-36-9	Si	B	6.0×10^4	6.8×10^2	.5% B_2H_6 in 10% SiH_4	
A-34-5	Si	P,B	1.3×10^4	1.3×10^3	.1% B_2H_6 in 10% SiH_4 (p-type) 10% SiH_4 (i) 1% PH_3 in 10% SiH_4 (n-type)	
			$a\text{-}Si_xC_{(1-x)}$(II)			
A-25-2	$Si_xC_{(1-x)}$		2.3×10^{11}	2.5×10^6	3.2% SiH_4, 6.8% C_2H_4	
A-25-5	$Si_xC_{(1-x)}$		1.6×10^{11}	9.0×10^6	3.2% SiH_4, 6.8% C_2H_4	
A-25-8	$Si_xC_{(1-x)}$		2.3×10^{11}	2.8×10^6	3.2% SiH_4, 6.8% C_2H_4	Remainder H_2 + Ar
A-26-2	$Si_xC_{(1-x)}$		3.0×10^9	5.0×10^4	9.5% SiH_4, .5% C_2H_4	Remainder H_2 + Ar
A-26-3	$Si_xC_{(1-x)}$		2.1×10^9	6.7×10^4	9.5% SiH_4, .5% C_2H_4	Remainder H_2 + Ar
A-12-3	$Si_xC_{(1-x)}$	B	8.8×10^7	5.8×10^7	1% B_2H_6 in 32% SiH_4, 68% C_2H_4	
A-12-7	$Si_xC_{(1-x)}$	B	8.4×10^7	6.4×10^7	1% B_2H_6 in 32% SiH_4, 68% C_2H_4	
			$a\text{-}Si_xGe_{(1-x)}$(ii)			
A-37-5	$Si_xGe_{(1-x)}$		2.3×10^{10}	1.0×10^6	50% SiH_4, 1% GeH_4	Remainder Ar
A-37-9	$Si_xGe_{(1-x)}$		9.6×10^{10}	2.4×10^6	50% SiH_4, 1% GeH_4	Remainder Ar
A-38-3	$Si_xGe_{(1-x)}$		6.5×10^9	1.2×10^5	20% SiH_4, 1.6% GeH_4	Remainder Ar
A-38-9	$Si_xGe_{(1-x)}$		1.2×10^9	1.1×10^5	20% SiH_4, 1.6 GeH_4	Remainder Ar

* Gas Flow 10 SCCM

REFERENCES

1. D. A. Anderson and W. E. Spear, Phil. Mag. 35, 1 (1977).
2. M. LeContellex, J. Richard, A. Guivarc'h, E. Ligeon and J. Fontenille, Thin Solid Films, to be published.
3. H. Matsunami, H. Masahiro, and T. Tanaka, J. Electron Mats. 8, 3 (1979).
4. H. Wieder, M. Cardona and C. R. Guarnieri, phys. stat. sol.(b) 92, 99 (1979).
5. A. Guivarc'h, J. Richard, M. LeContellec, E. Ligeon and J. Fontenille, submitted to J. Appl. Phys.
6. J. Chevallier, H. Wieder, A. Onton and C. R. Guarnieri, Solid St. Comms 24, 867 (1977).
7. D. E. Carlson, Abstract No. 11.2, Technical Digest of the International Electron Devices Meeting, IEEE, Washington, DC, 214 (1977).
8. M. C. Cretella, Quarterly Report, Contract No. DE-AC03-79ET20460.
9. M. A. Paesler, D. A. Anderson, E. C. Freeman, G. Moddel, William Paul, Phys. Rev. Lett. 41, 1492 (1978).
10. J. C. Knights, G. Lucovsky and R. J. Nemanich, To be published.
11. R. W. Griffith, Abstract, Contractor's Review Meeting, Contract No. EY-76-C-02-0016, Princeton, NJ, May 30, 1979.
12. W. Paul, private communication.
13. J. C. Knights, Quarterly Report, Contract No. 03-79-ET-23033, April 30, 1979.
14. L. D. Partain and S. P. Shea, Abstract No. P1-3, Photovoltaic Solar Energy Conference, Berlin (West) Germany, April 23, 1979.
15. D. L. Staebler, C. R. Wronski, Appl. Phys. Letters 31, 292 (1977).
16. W. E. Spear, P. G. LeComber, Phil. Mag. 33, 935 (1976).
17. W. E. Spear, Adv. Phys. 26, 811 (1977).

FIGURE CAPTIONS

Figure No.

1. Change in Eog with composition: (a) a-Si_xC_{1-x}(H), diluted to 10% with H_2 + Ar; (b) a-Si_x-Ge_{1-x}(H), variable dilution with argon only.

2. Geometry of coplanar contact samples used for resistivity measurements.

3. I vs. V characteristic of coplanar contact sample, p-doped a-Si(H).

4. I vs. V characteristic of coplanar contact sample at different illumination levels; (FL) = fluorescent light; (D) = dark. Sample is layered n-i-p a-Si(H).

5. (a) I vs. V characteristic of coplanar contact sample. (b) V vs. d across sample with 5 volts applied. (c) V vs. d across sample with 25 volts applied. Sample is p-doped a-Si(H).

6. V vs. d across undoped a-Si(H) at different illumination levels.

7. Conductivity vs. 1000/T(^oK) for undoped a-Si(H) at different illumination levels. Note hysteresis.

8. Conductivity vs. 1000/T for n-doped a-Si(H).

9. Conductivity vs. 1000/T for undoped a-Si_xC_{1-x}(H). Gas volume ratio C/Si = 0.13.

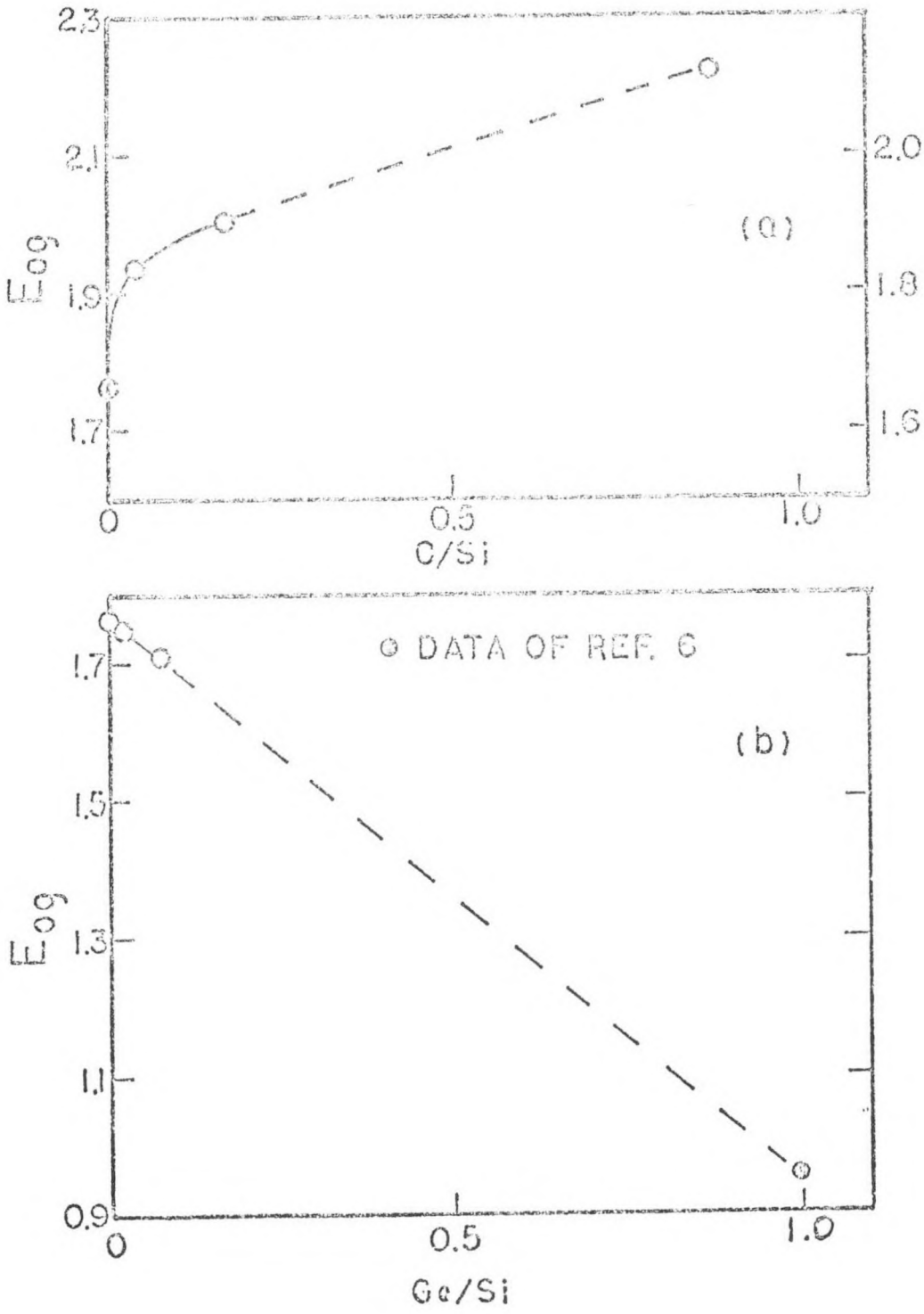
2.3
2.1
1.9
1.7
Eg eV
2.0
1.8
1.6
(a)
0
0.5
1.0
C/Si
o DATA OF REF. 6
(b)
1.7
1.5
1.3
1.1
0.9
Eg eV
0
0.5
1.0
Ge/Si

Fig. 1

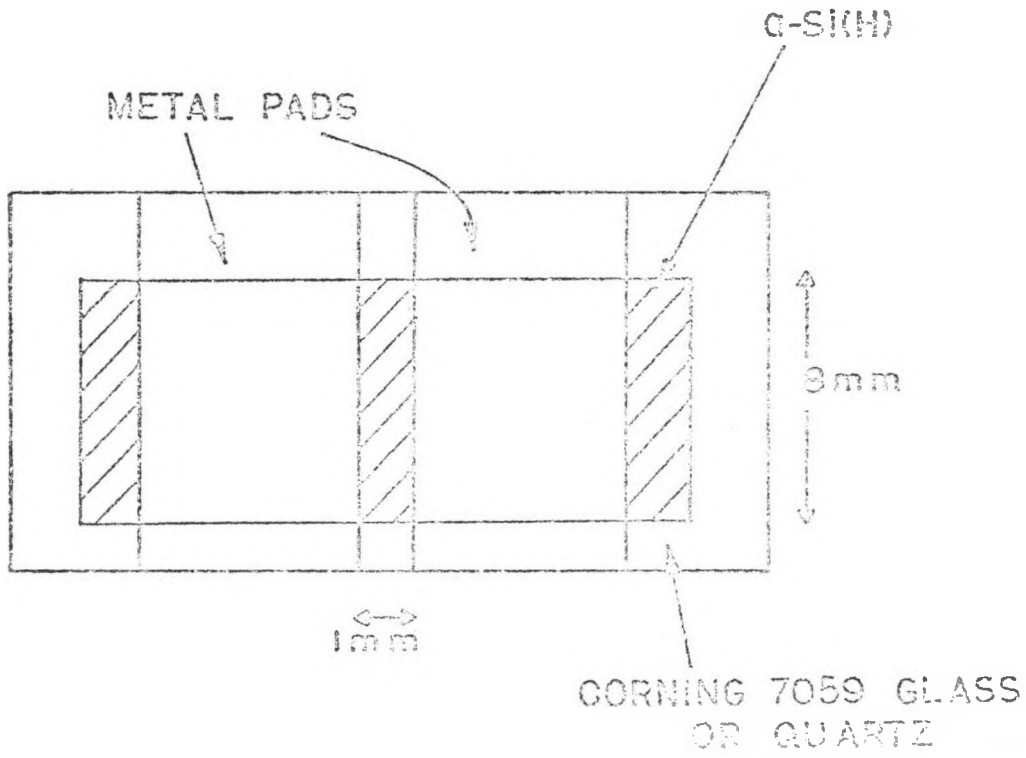

Fig. 2

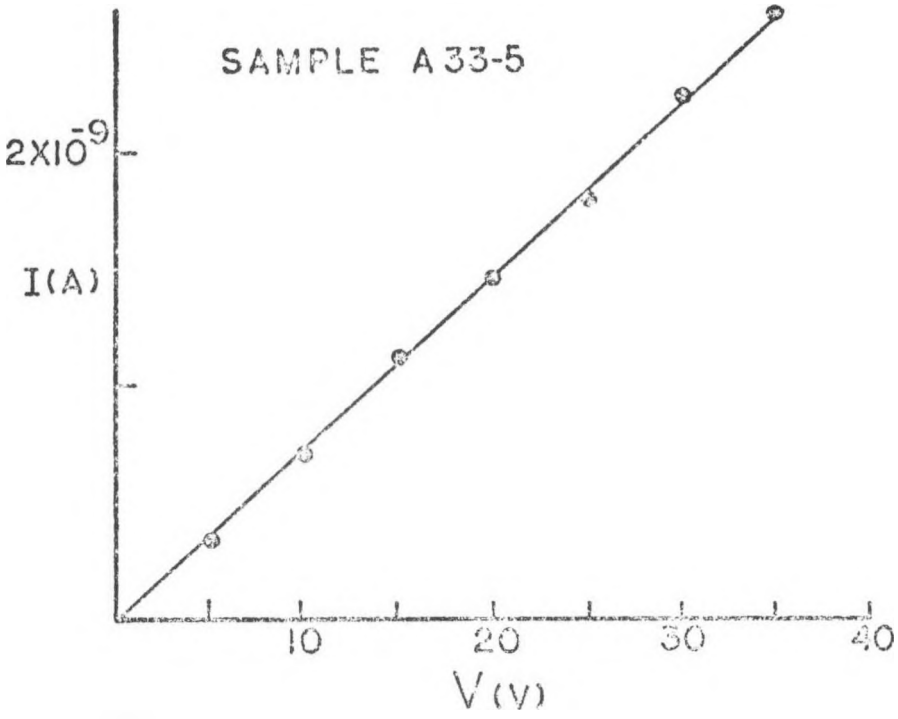
SAMPLE A33-5
2X10⁻⁹
I(A)
10
20
30
40
V(V)

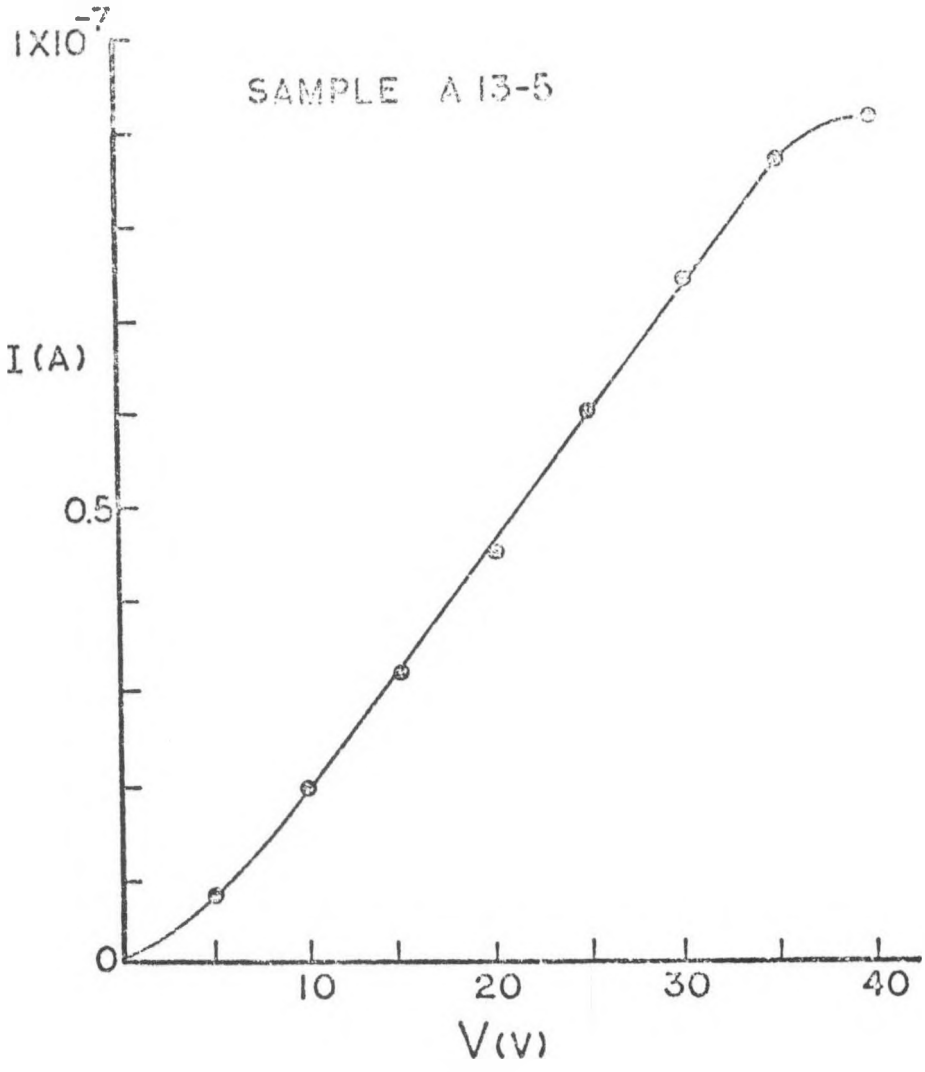
1X10⁻⁷
SAMPLE A13-5
I(A)
0.5
0
10
20
30
40
V(V)

Fig. 3

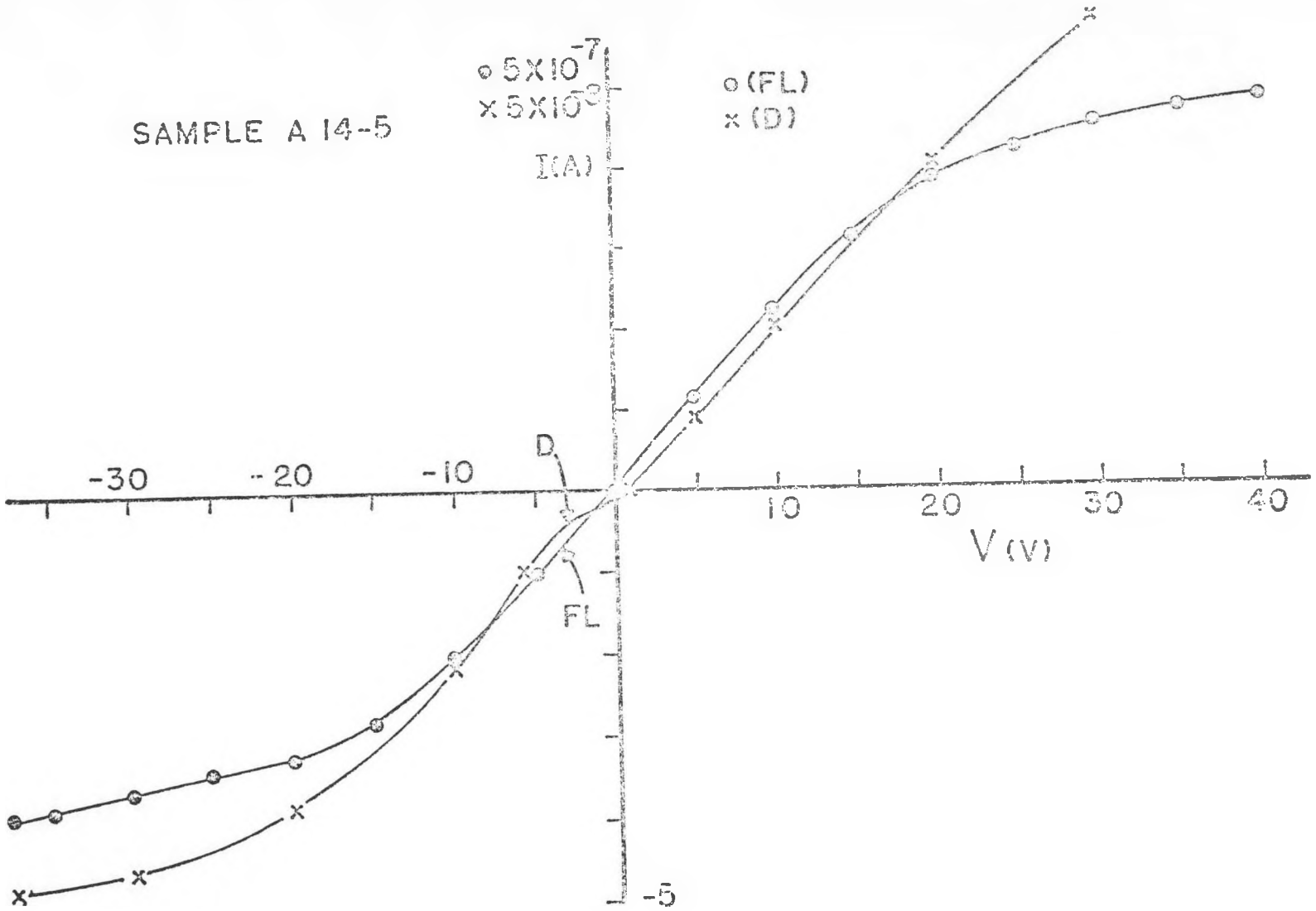

Fig. 4

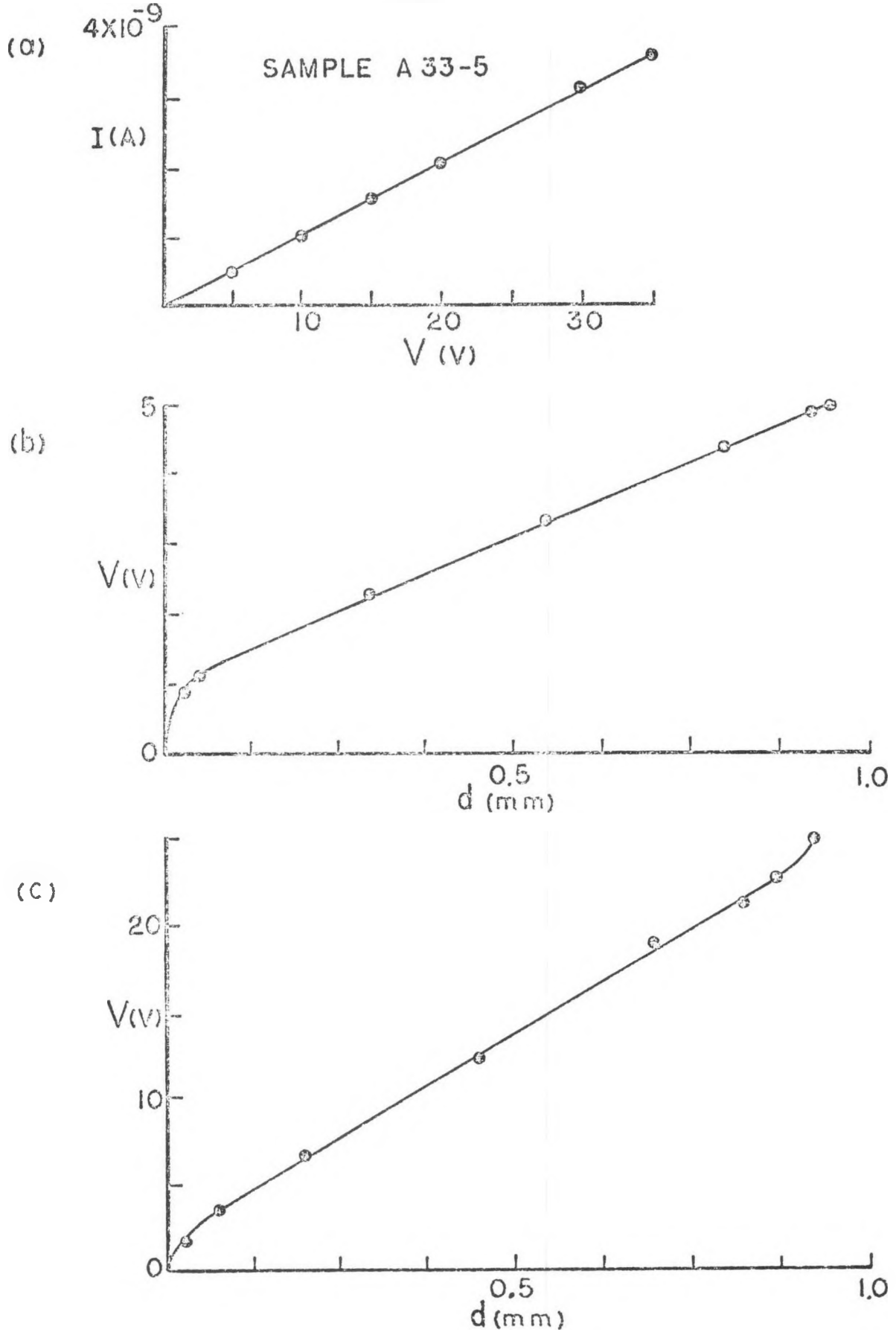
(a)
4X10⁻⁹
SAMPLE A 33-5
I(A)
10
20
30
V (V)
(b)
5
V(V)
0
0.5
1.0
d (mm)
(c)
20
V(V)
10
0
0.5
1.0
d (mm)

Fig. 5

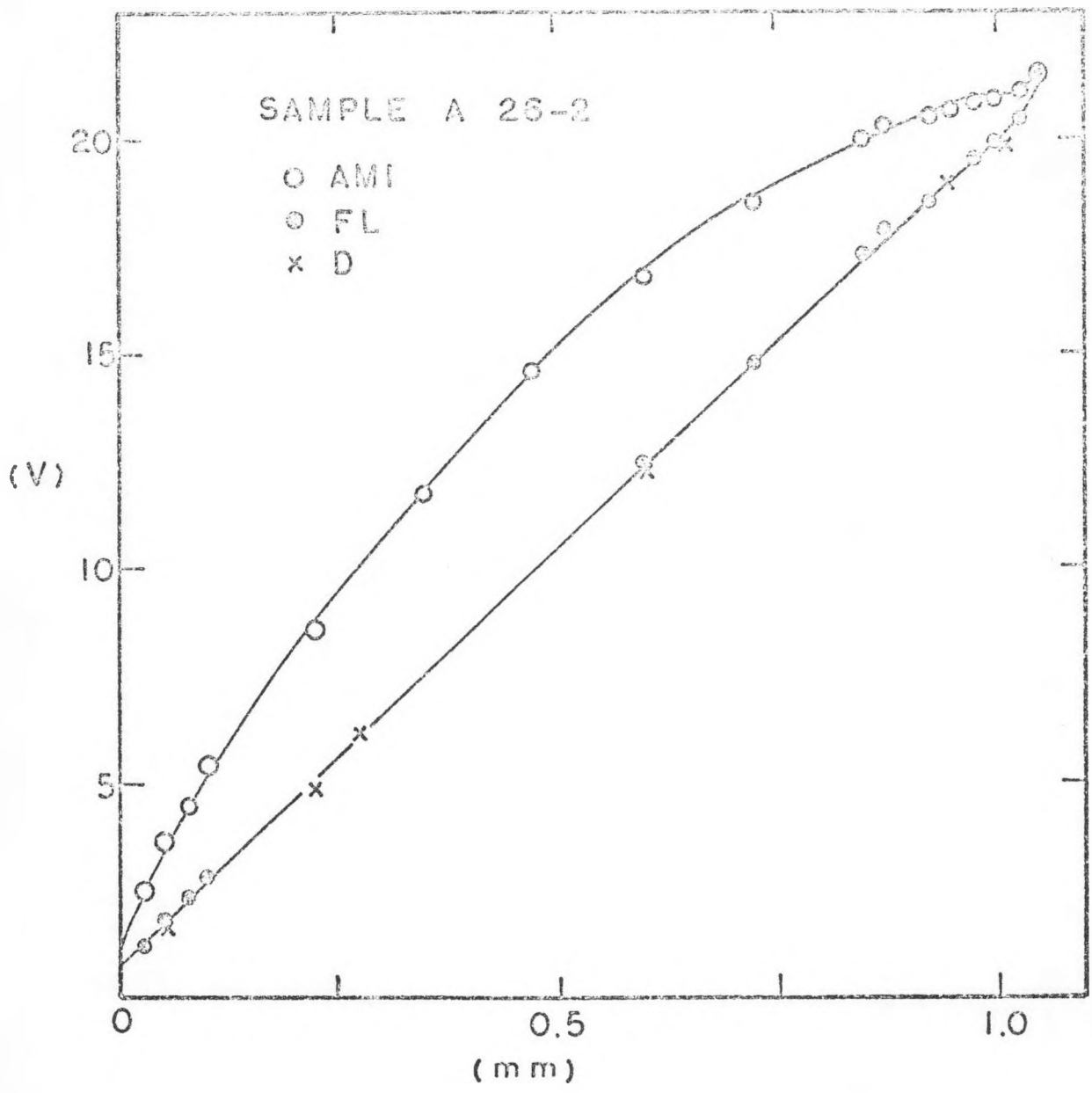

Fig. 6

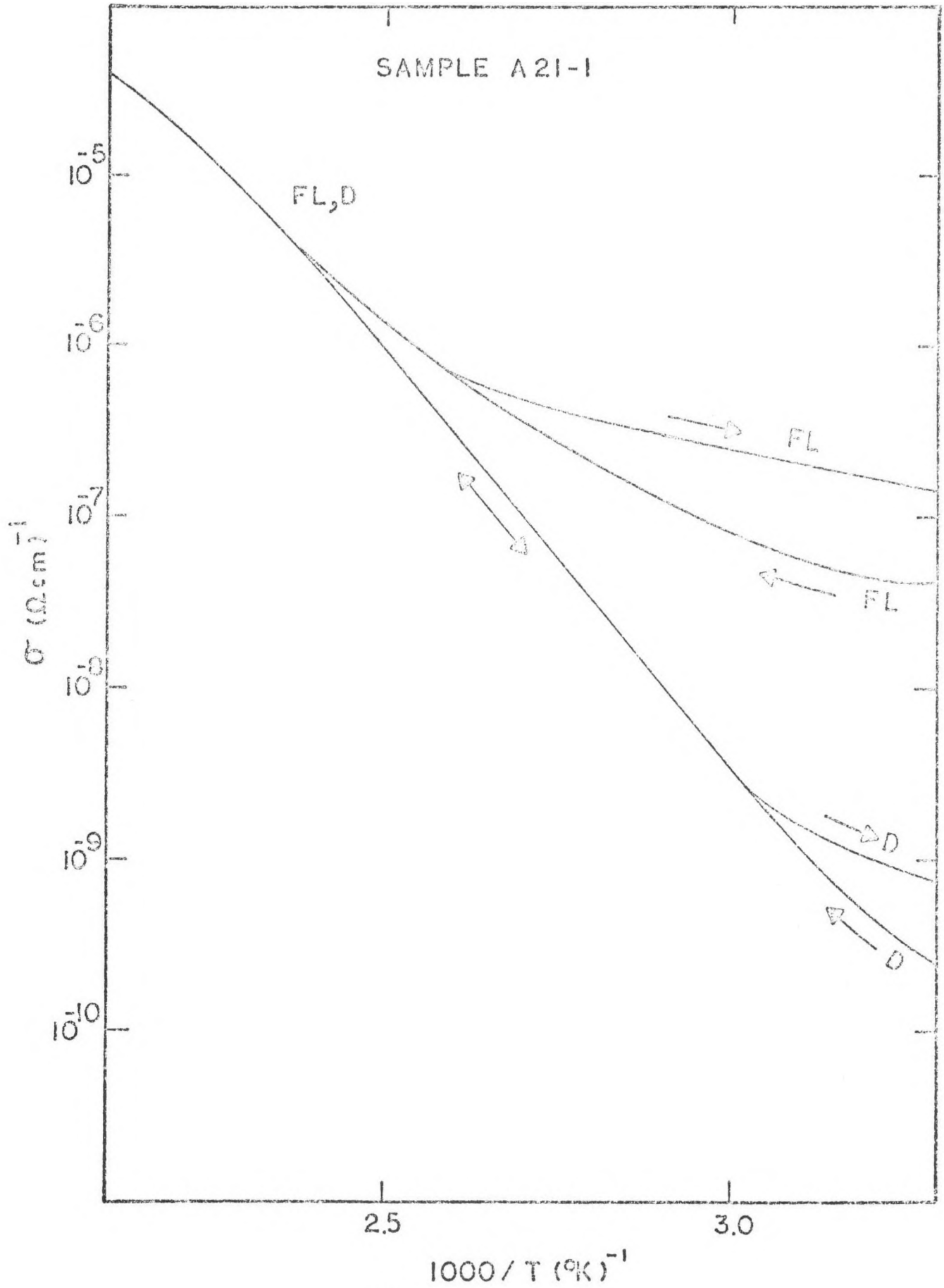
SAMPLE A 21-1
FL,D
FL
FL
D
D
10^{-5}
10^{-6}
10^{-7}
10^{-8}
10^{-9}
10^{-10}
$\sigma\ (\Omega cm)^{-1}$
2.5
3.0
1000 / T (°K)$^{-1}$

Fig. 7

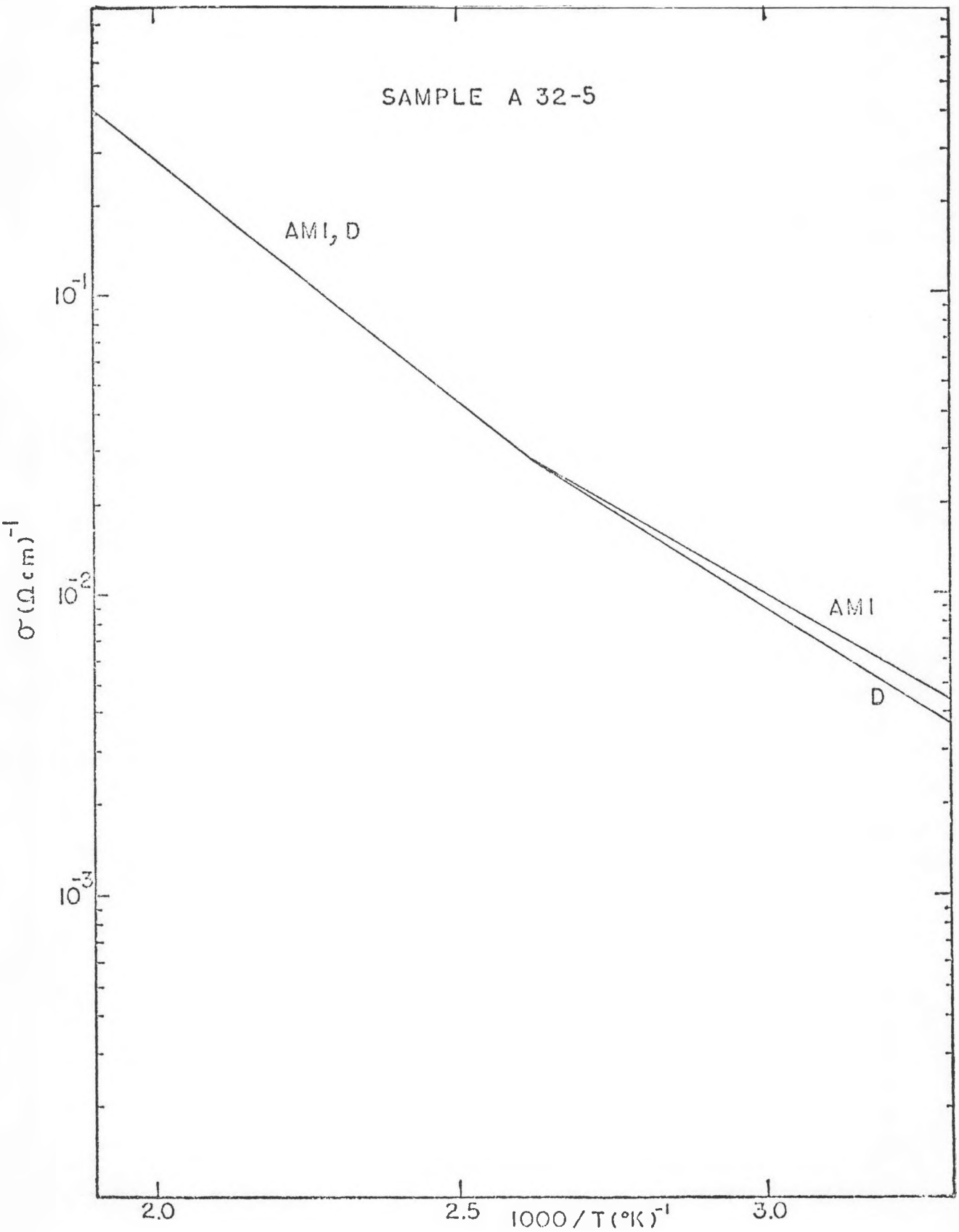
SAMPLE A 32-5
AM1, D
AM1
D
10^{-1}
10^{-2}
10^{-3}
$\sigma\,(\Omega\,cm)^{-1}$
2.0
2.5
3.0
1000 / T (°K)$^{-1}$

Fig. 8

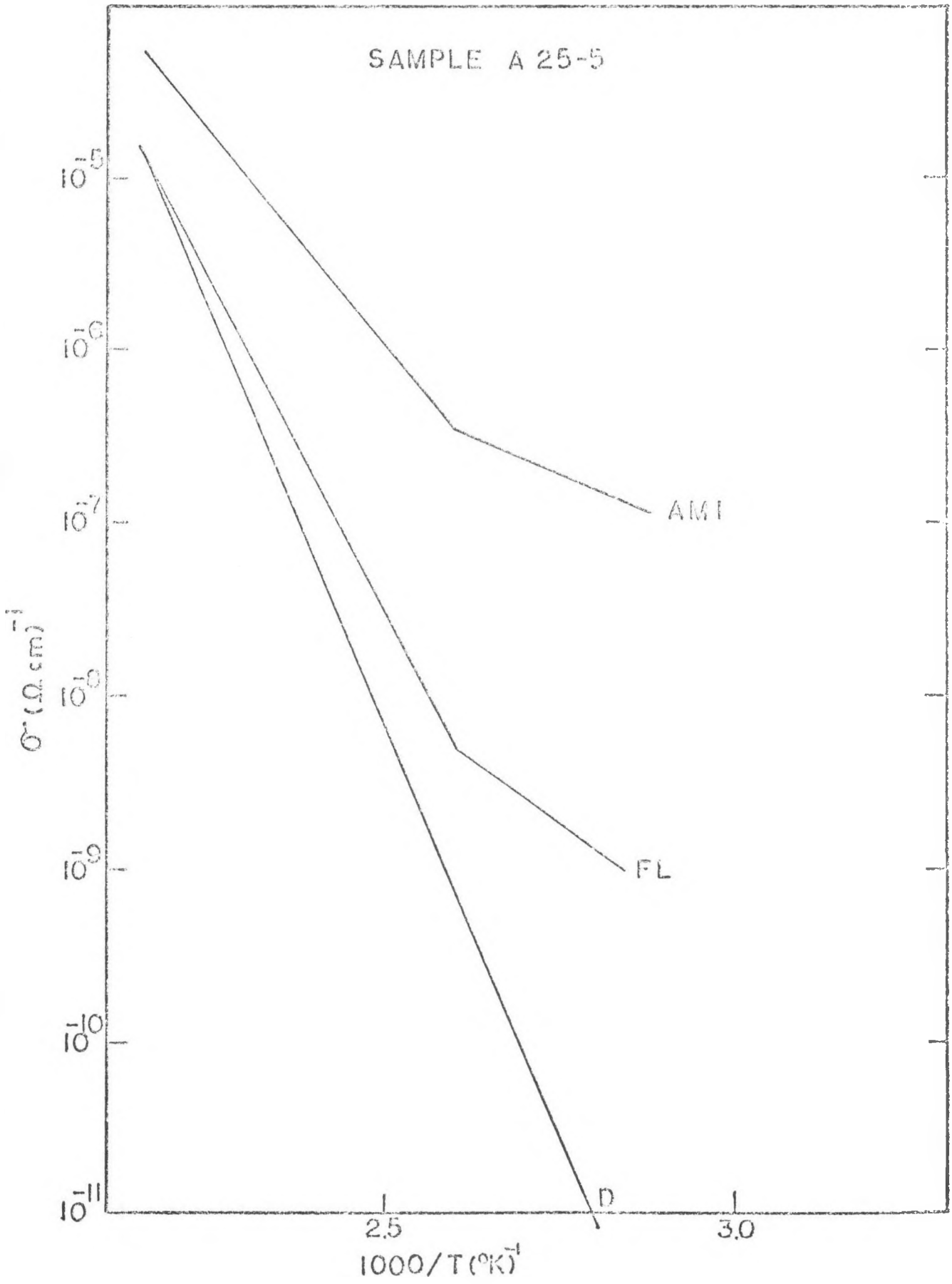
SAMPLE A 25-5
AM
FL
D
10^{-5}
10^{-6}
10^{-7}
10^{-8}
10^{-9}
10^{-10}
10^{-11}
σ (Ω cm)$^{-1}$
2.5
3.0
1000/T (°K)$^{-1}$

Fig. 9

APPENDIX

Calculation of Optical Constants (near the absorption edge) in Amorphous Films

The following is a straightforward approach to the approximate evaluation of the optical constants for thin films. It is assumed that the film is of uniform composition through its thickness and that the thickness is indeed well defined. Lack of uniform composition will probably not be too serious for this first cut procedure, however.

The results presented here will be for a film deposited on either SiO_2 substrates ($n = 1.54$ at $\sim.5\mu$) or 7059 glass ($n = 1.53$ at $\sim.5\mu$). This ensures that the index of refraction of the film is always greater than that of the substrate. The thickness must be known.

A. Obtaining the Index of Refraction

$T_{obs}(\lambda)$ should look like the curve below. Generally, $T_{obs}(\lambda) \to 1.0$ for long λ.

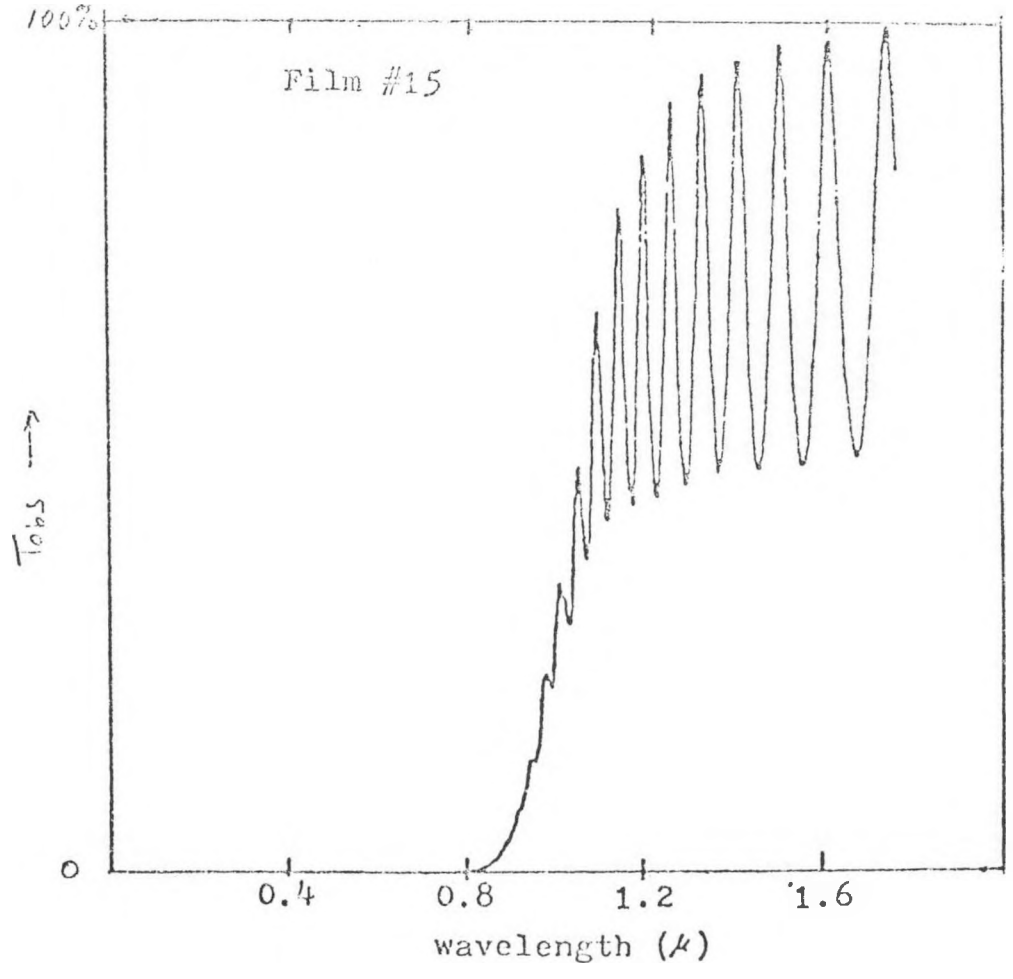

The oscillations in T_{obs} at long λ are due to interference effects. The slowly changing (with wavelength) value of n can be obtained from the spectral location of any two adjacent interference maxima (or minima)

$$n = \frac{1}{2d}\left(\frac{\lambda_1 \lambda_2}{\lambda_1 - \lambda_2}\right)$$

where d is the sample thickness. If several maxima and minima are present, an average value for n can be obtained (this assumes no dispersion, of course). The equation can also be written

$$n = \frac{1}{2d\ (k_2 - k_1)}, \quad \text{where} \quad k = \frac{1}{\lambda}$$

It is suggested that maxima and minima which are "damped" in the short wavelength region not be used to get n since they may be shifted by the rapidly decreasing T. Armed with an average value of n obtained from λ where $T_{obs\ max} \approx 1$, the value of the absorption coefficient can be obtained.

B. Calculation of the Absorption Coefficient (α)

We have been doing this two approximate ways (getting good agreement), but the more general of the two is that of Freeman and Paul.† They assume multiple incoherent reflections in both the film and the substrate. Thus, this approximation is strictly valid for the highly absorbing spectral region (shorter wavelengths) where interference fringes do not occur. We abbreviate T_{obs} as T :

$$\alpha = \frac{-1}{d} \ln \left| \frac{1}{B}\left\{A + \left[A^2 + 2BT\ (1 - R_2R_3)\right]^{1/2}\right\} \right|$$

where

$$A = -(1 - R_1)(1 - R_2)(1 - R_3)$$

$$B = 2T\ (R_1R_2 + R_1R_3 - 2R_1R_2R_3)$$

$$R_1 = \left(\frac{n - 1}{n + 1}\right)^2 \qquad R_2 = \left(\frac{n - n_o}{n + n_o}\right)^2 \qquad R_3 = \left(\frac{n_o - 1}{n_o + 1}\right)^2$$

and $n_o = 1.53$ for 7059 substrate or 1.54 for quartz.

† Freeman, E. C. and Paul, William, Phys. Rev. B18, 4288 (1978).

Note, the values in the "ln" expression tend to almost cancel out; thus, must individually be taken to several places (particularly the A and $[A^2 + 2\,BT\,(1 - R_2R_3)]^{\frac{1}{2}}$ terms). An example for film A-7-1 follows.

C. Homogeneity

As the wavelength is increased, the film can be expected to have a smaller absorption coefficient and T_{obs} should approach unity for the maxima. If it does not, the film probably does not have a uniform composition (the value of n changes through the thickness) or the sample has a rough surface that scatters the incident beam. We lean toward the latter possibility, however. If T_{obs} does equal unity at the interference maxima and if the film is of uniform composition, then the transmittance at the interference minima has a theoretical value:†

$$T_{obs}(\text{min}) \approx \left[1.0 - \left(\frac{n^2 - n_o}{n^2 + n_o}\right)^2\right] \left[1.0 - \left(\frac{1 - n_o}{1 \times n_o}\right)^2\right]$$

If T_{obs}(min) does not drop to this value within 1 or 2% (and we have seen only a few films that satisfy this, then the film is not homogeneous. Note, film A-7-1 is not "very" homogeneous, as shown in the example.

We are continuing to explore the approximations, etc., made above. In particular, we are examining predicted transmittance from the exact thin film formulae, the impact of assuming no dispersion, and the effect of non-homogeneity on calculated values of transmittance. This will lead to an exploration of multi-layer film theory. The above procedure, however, should suffice for present requirements.

---

† Yates, Douglas A., "Electron States in Amorphous Gallium Phosphide," (thesis) University Microfilms, Ann Arbor, MI, p. 136.

See also: Heavens, O. S., "Optical Constants in Thin Films," in Physics of Thin Films 2, Academic Press (1964), p. 204.

Sample Analysis: A-7-1

$$d = 0.34\mu = 0.34 \times 10^{-4} \text{ cm} \qquad \frac{1}{2 n_d} = k_2 - k_1$$

B.

k for T max		difference	n	confidence
18850 cm^{-1}	>	2800	5.25	
16050-16100	>	3650	4.03	best
12400	>	3850	3.82	best
8550	>	4050	3.63	
-4500				

$$\boxed{n_{ave} = 3.9}$$

C. $R_1 = .3503$ $R_2 = .1905$ $R_3 = .0439$

$A = -.5028$ $B = .1525\ T$

$$\alpha = -\frac{1}{d} \ln \left| \frac{1}{.1525\ T} \left\{ .5028 + \left[.252808 + .3024\ T^2 \right]^{\frac{1}{2}} \right\} \right|$$

$\lambda(\mu)$	T	$\alpha(cm^{-1})$	$h\nu$(eV)	$\alpha h\nu$
.450	.050	6.82×10^4	2.76	434
.460	.090	5.09×10^4	2.70	371
.475	.165	3.33×10^4	2.61	295
.500	.290	1.72×10^4	2.48	207

D. Homogeneity? at long λ ($\lambda > .8\mu$), $T_{obs} = 1.0 \pm .01$

using formula for $T_{obs}(min)$, with $n = 3.9$, $n_o = 1.53$

$T_{obs}(min) = .35$, theoretically for homogeneity.

Experimentally, we get .61, at best (near .7μ)

Thus, film is <u>not</u> homogeneous.

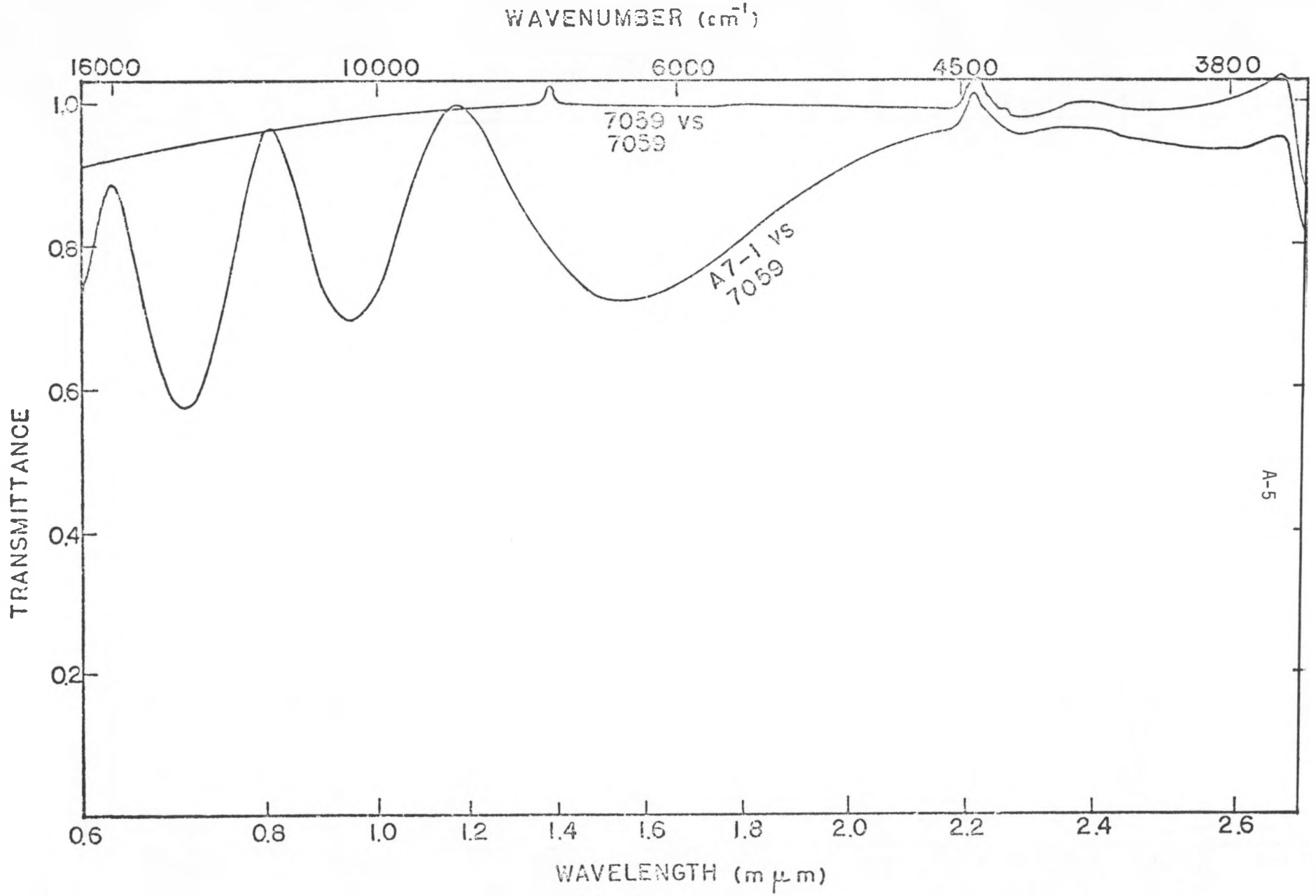
WAVENUMBER (cm⁻¹)
16000
10000
6000
4500
3800
1.0
0.8
0.6
0.4
0.2
TRANSMITTANCE
7059 vs
7059
A7-1 vs
7059
A-5
0.6
0.8
1.0
1.2
1.4
1.6
1.8
2.0
2.2
2.4
2.6
WAVELENGTH (mμm)

Fig. A-1

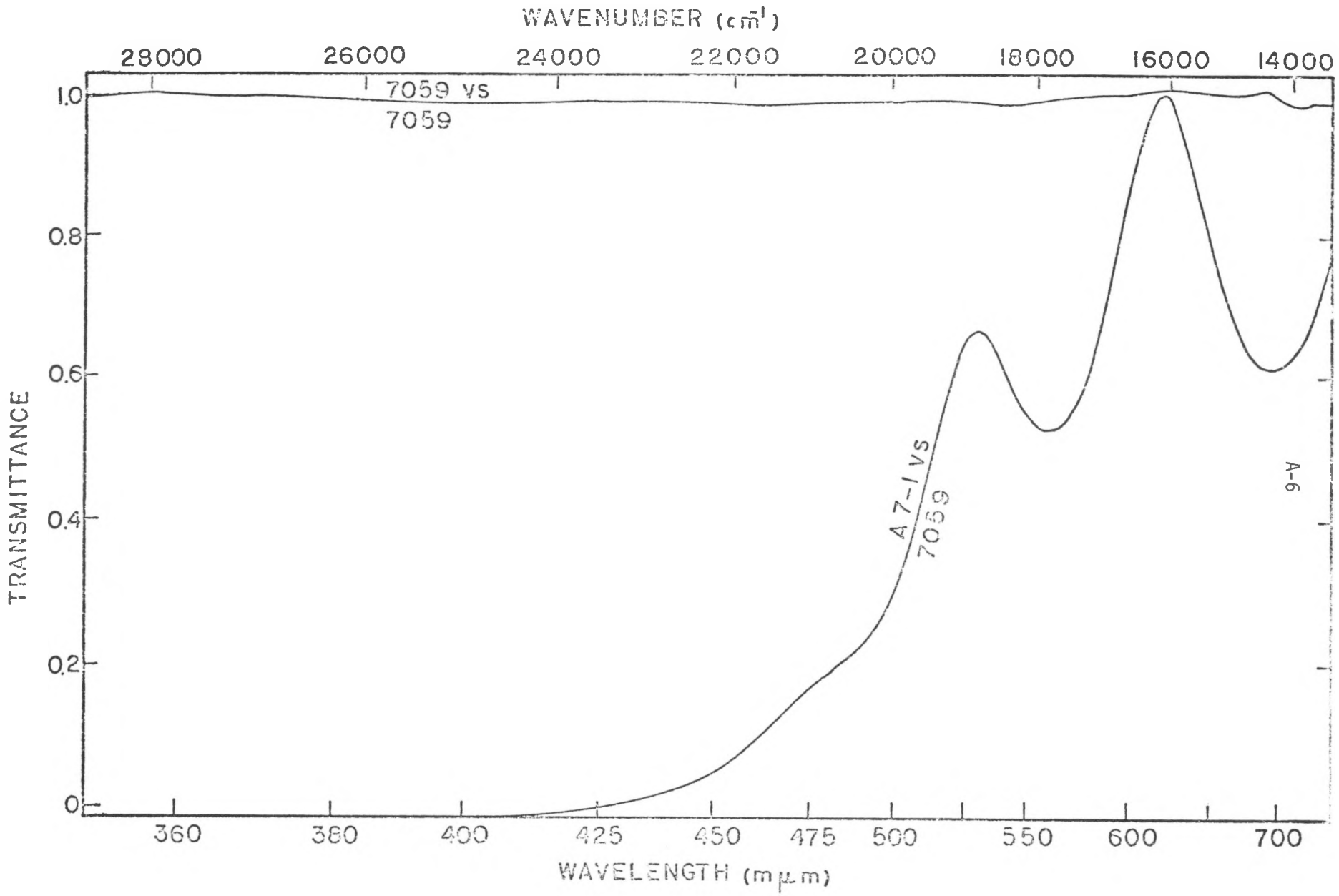
WAVENUMBER (cm⁻¹)
28000
26000
24000
22000
20000
18000
16000
14000
7059 vs
7059
A7-1 vs
7059
A-6
TRANSMITTANCE
1.0
0.8
0.6
0.4
0.2
0
360
380
400
425
450
475
500
550
600
700
WAVELENGTH (mμm)

Fig. A-2

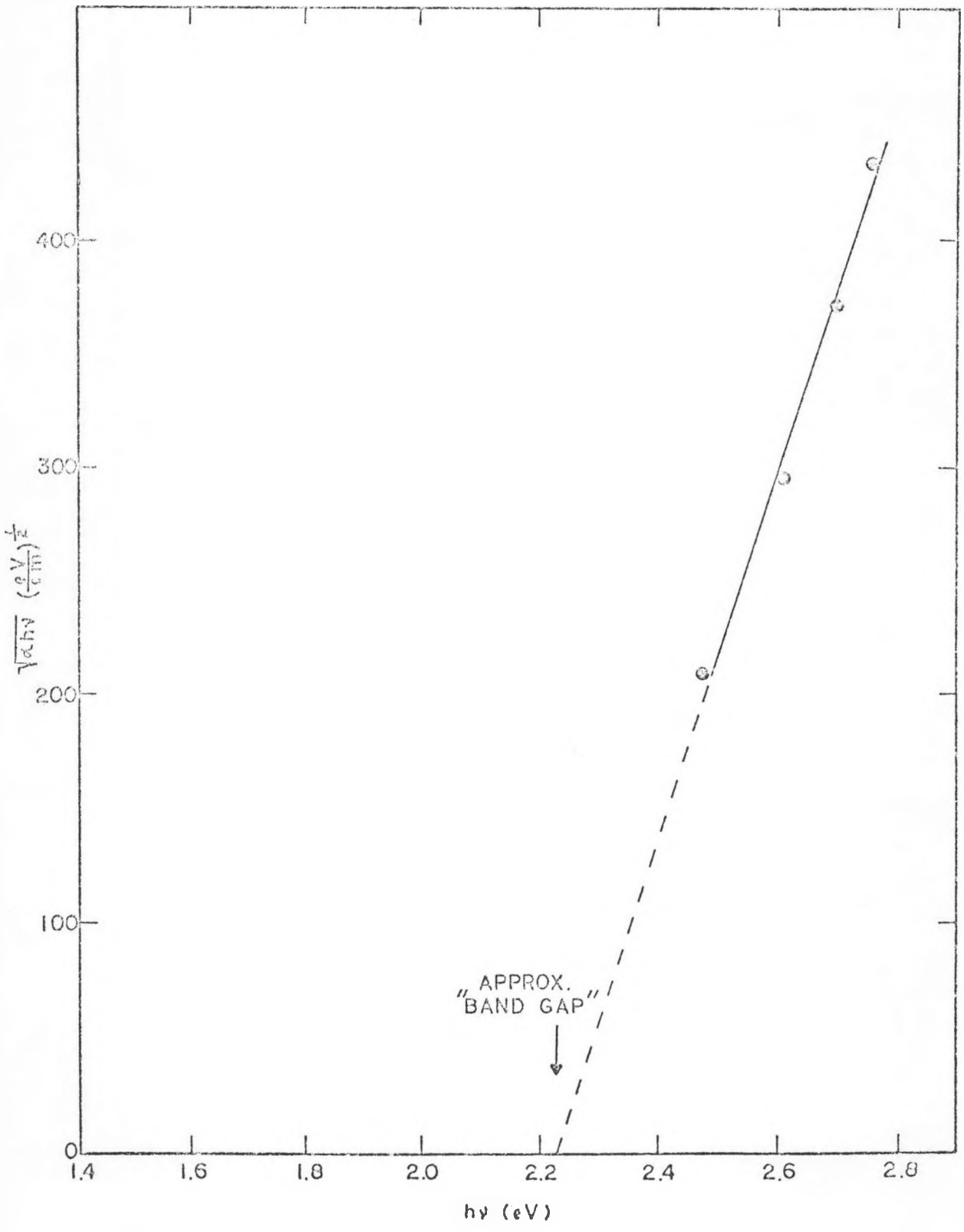

Fig. A-3

☆U.S. GOVERNMENT PRINTING OFFICE: 1979-640-258-1644